

Spectral mineralogy of terrestrial planets: scanning their surfaces remotely

ROGER G. BURNS

Department of Earth, Atmospheric and Planetary Sciences, Massachusetts Institute of Technology, Cambridge, Massachusetts 02139, USA

Abstract

Spectral measurements of sunlight reflected from planetary surfaces, when correlated with experimental visible–near-infrared spectra of rock-forming minerals, are being used to detect transition metal cations, to identify constituent minerals, and to determine modal mineralogies of regoliths on terrestrial planets. Such remote-sensed reflectance spectra measured through earth-based telescopes may have absorption bands in the one micron and two micron wavelength regions which originate from crystal field transitions within Fe^{2+} ions. Pyroxenes with Fe^{2+} in $M2$ positions dominate the spectra, and the resulting $1\ \mu\text{m}$ versus $2\ \mu\text{m}$ spectral determinative curve is used to identify compositions and structure-types of pyroxenes on surfaces of the Moon, Mercury, and asteroids, after correcting for experimentally-determined temperature-shifts of peak positions. Olivines and Fe^{2+} -bearing plagioclase feldspars also give diagnostic peaks in the $1\ \mu\text{m}$ region, while tetrahedral Fe^{2+} in glasses absorb in the $2\ \mu\text{m}$ region as well. Opaque ilmenite, spinel and metallic iron phases mask all of these Fe^{2+} spectral features. Laboratory studies of mixed-mineral assemblages enable coexisting Fe^{2+} phases to be identified in remote-sensed reflectance spectra of regoliths. Thus, noritic rocks in the lunar highlands, troctolites in central peaks of impact craters such as Copernicus, and high-Ti and low-Ti mare basalts have been mapped on the Moon's surface by telescopic reflectance spectroscopy. The Venusian atmosphere prevents remote-sensed spectral measurements of its surface mineralogy, while atmospheric CO_2 and ferric-bearing materials in the regolith on Mars interfere with pyroxene characterization in bright- and dark-region spectra. Reflectance spectral measurements of several meteorite types, including specimens from Antarctica, are consistent with a lunar highland origin for achondrite ALHA 81005 and a martian origin for shergottite EETA 79001, although source regions may not be outermost surfaces of the Moon and Mars. Correlations with asteroid reflectance spectra suggest that Vesta is the source of basaltic achondrites, while wide ranges of olivine/pyroxene ratios are inconsistent with an ordinary-chondrite surface composition of many asteroids. Visible–near-infrared spectrometers are destined for instrument payloads in future spacecraft missions to neighbouring solar system bodies.

“... Scientific study (of planets and asteroids in the next half century) probably will be based largely on remote observations As orbiting telescopes are developed with facilities for observation without loss of spectral range in the Earth's atmosphere, many ideas of the mineralogy of the surface of solar-system bodies should be tested.”

J. V. Smith (1979)

In: The Hallimond Lecture for the Centenary of the Mineralogical Society, *Mineral. Mag.* **43**, 4.

KEYWORDS: reflectance spectroscopy, terrestrial planets, scanning.

Historical background

It is fitting that this, the 19th Hallimond Lecture, should have as its central theme reflectance spectroscopy of minerals because A. F. Hallimond, himself, was particularly interested in reflectance

properties of minerals (Hallimond, 1956). He did much to revolutionize microscope design and to systematize reflected light microscopy and the optics of absorbing crystals (Smith, 1969). Hallimond would have been intrigued by present-day technology that is being used to measure and

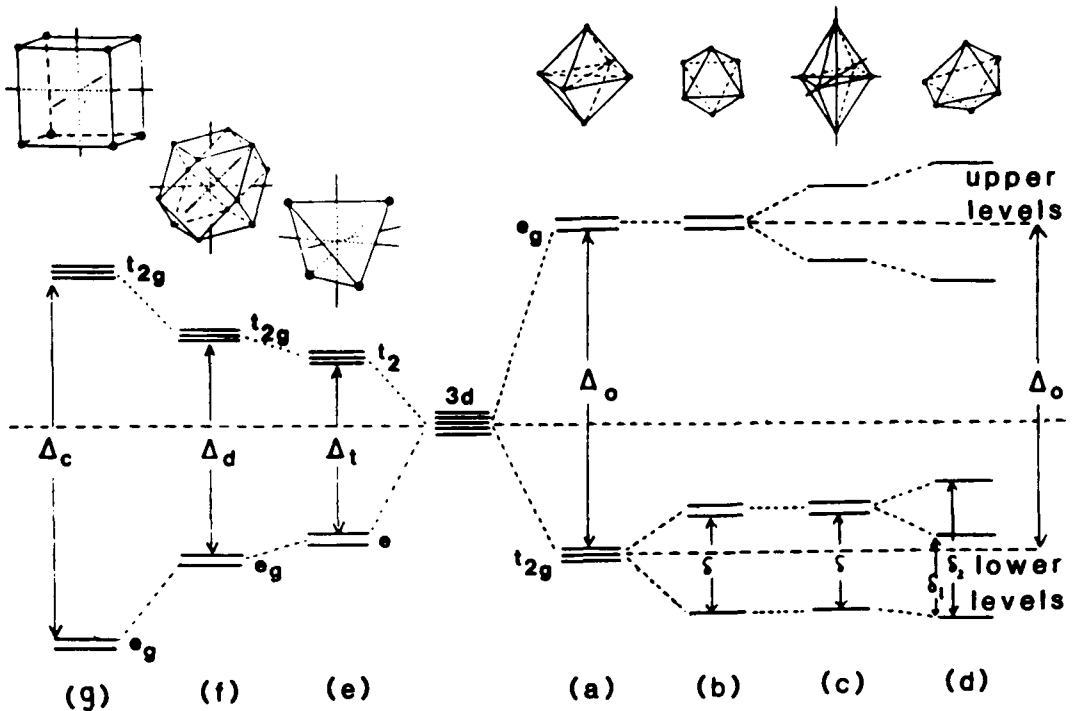


FIG. 1. Relative energies of 3-*d* orbitals of a transition metal ion in different coordination environments (modified from Burns, 1985). (a) regular octahedron (e.g. ~pyroxene *M1* site; basaltic glass); (b) trigonally distorted octahedron (e.g. ~olivine *M2* site; spinel); (c) tetragonally distorted octahedron (e.g. ~olivine *M1* site); (d) very distorted six-coordination site (e.g. pyroxene *M2* site); (e) tetrahedral site (e.g. spinel; basaltic glass); (f) dodecahedral site (e.g. ~perovskite *A*-site); (g) cubic site (e.g. ~garnet). Note that the 3-*d* orbitals are separated into widely spaced energy levels in the pyroxene *M2* site, and these splittings are responsible for the 1 μm and 2 μm spectral features for Fe^{2+} ions.

interpret reflectance properties of minerals on surfaces of planets remote from the petrographic microscope.

The field of mineral spectroscopy has truly come of age, as is being witnessed by the diversity of techniques and applications being described at this, the First Winter Conference of the Mineralogical Society on Spectroscopic Studies of Minerals. It was just 21 years ago that the author gave his inaugural lecture to the Society on the topic of electronic spectra of orthopyroxenes and addressed the conspicuous problem of why orthopyroxenes in granulite facies metamorphic rocks display distinctive red-green pleochroism (Burns 1966a). Following in the Hallimond tradition, these papers heralded two major breakthroughs in spectral mineralogy (Burns, 1970). First, polarizing microscopes equipped with universal stage attachments inserted inside conventional spectrophotometers enabled polarized absorption spectral measurements to be made on oriented phenocrysts and porphyroblasts in rock thin sec-

tions, as well as gem-sized crystals (Burns, 1966b). Second, crystal field theory was being used for the first time to interpret optical spectra of rock-forming silicates (Burns, 1965; White and Keester, 1966). This dual approach to mineral spectroscopy has continued during the past two decades; on the one hand, interpretations of the visible-near-infrared spectra of pyroxenes and olivines have been further refined (Bancroft and Burns, 1967; Runciman *et al.*, 1973a,b; Burns, 1974, 1985; Goldman and Rossman, 1977; Steffen *et al.*, 1988), while on the other hand, ranges of experimental measurements have been extended to different compositions, pressures and temperatures (Mao and Bell, 1973; Abu-Eid, 1976; Hazen *et al.*, 1977, 1978; Parkin and Burns, 1980; Burns, 1982), propelled by the need to better understand surfaces of terrestrial planets and their interiors.

It was also just 20 years ago that pioneering measurements of remote-sensed mineral spectral data for the Moon and Mars were first reported (Adams, 1968; McCord and Adams, 1969). Sunlit

surfaces of these planets reflect light, the spectral features of which, when measured through Earth-based telescopes, may be identified by comparisons with reference spectra of rock-forming minerals (Adams, 1974, 1975). Major developments in design and resolution of telescopes and radiation detector technology have rocketed the field of remote-sensed spectral mineralogy into pre-eminence in present-day research of planetary materials and future planned space missions (McCord, 1988).

Many of the developments in spectral mineralogy applied to planetary geochemistry have been initiated over the years by fellow student and colleague investigators, first at Oxford University and later at MIT, and their contributions are acknowledged throughout this presentation. Each terrestrial planet has spawned its own unique set of problems which have had to be solved in order to better understand the mineral assemblages contributing to remote-sensed reflectance spectra scattered from its surface. Selected examples are described here and set the theme developed throughout the paper. First, origins of electronic transitions in iron-bearing minerals, which are induced by visible-near infrared radiation from the Sun, are discussed. Reflectance spectra of the Moon are then described together with laboratory investigations on mineral mixtures. Effects of temperature on crystal field spectra are considered next, because they refine interpretations of lunar spectra and set constraints on mineral constituents of the surface of Mercury. The need to understand spectral features arising from oxidative weathering products of mafic igneous rocks underlies interpretations of remote-sensed spectra of Venus and Mars, which are also complicated by atmospheric absorption at critical wavelengths. Finally, the information that spectral measurements of meteorites brings to bear on the mineralogy of terrestrial planets is discussed. The coverage, therefore, is more focused than the space-time voyage of planetary mineralogy addressed during the Hallimond Lecture for the 1976 centenary of the Mineralogical Society (Smith, 1979).

The central theme developed in this presentation is that essentially everything we know about the surface mineralogy of terrestrial planets, except for the Earth, the Moon and, perhaps, Mars, has resulted from reflectance spectroscopy used as a remote-sensing tool and with earth-based telescopes. The focus is optical spectral measurements of pyroxenes, and to a lesser extent olivine, because these minerals are so diagnostic of the evolution of terrestrial planets.

Origin of visible–near-infrared spectra

The first-series transition elements Fe and Ti, and to a lesser extent Cr and Mn, are responsible for spectral features of pyroxenes and olivines in the wavelength range 0.33–2.50 μm (i.e. 330–2500 nm or 33 000–4000 cm^{-1}). These optical spectra result from excitations of electrons between energy levels of unfilled 3-*d* orbitals induced by the crystal field of oxygen anions surrounding the transition metal cation in its coordination site in the pyroxene or olivine structures (Burns, 1970, 1985). The schematic energy level diagrams shown in Fig. 1 demonstrate that relative energies and separations of t_{2g} and e_g orbital groups are strongly influenced by the symmetry and distortion of the coordination environment about a transition metal ion. Of prime significance to planetary remote-sensed spectra described later are the splittings of 3-*d* orbital energy levels for Fe^{2+} ions in highly distorted pyroxene *M2* sites. Whereas the pyroxene *M1* site is almost a regular octahedron and the olivine *M1* and *M2* sites approximate tetragonally-distorted and trigonally-distorted octahedra, respectively, these coordination polyhedra are not as puckered as the pyroxene *M2* site. As a result Fe^{2+} cations not only are strongly enriched in pyroxene *M2* sites, but they also produce two intense and widely separated absorption bands in the vicinity of 1 μm and 2 μm . These diagnostic pyroxene spectral features are illustrated in Fig. 2 by the polarized absorption spectra for single crystals of pyroxenes from several Moon rocks and in Fig. 3 by the diffuse reflectance spectra of powdered lunar mineral samples. Note the inverted relationship of spectral features between absorption (transmission) spectra and reflectance spectra, as well as the poorer resolution of the diffuse reflectance spectra. The crystal field transitions portrayed by these spectra are to the upper levels of split e_g orbitals, which are most widely separated for Fe^{2+} in pyroxene *M2* sites (cf. Fig. 1). Octahedrally coordinated Fe^{2+} ions in all ferromagnesian silicates give rise to crystal field bands in the 1 μm region, the positions and intensities of which serve to identify these phases in diffuse reflectance spectra of powdered rocks and surfaces of planets (Burns *et al.*, 1972*a,b*; Adams, 1974, 1975; Burns and Vaughan, 1975; Vaughan and Burns, 1977). Lunar calcic plagioclase feldspars, which contain small amounts of Fe^{2+} replacing Ca^{2+} ions in large coordination sites, produce a weak crystal field band centered around 1.20 μm (Fig. 3*a*). The 1.05 μm band in olivine spectra (Fig. 3*d*) originates from Fe^{2+} ions in *M2* sites, while Fe^{2+} ions in *M1* sites produce the features at c. 0.85 μm and

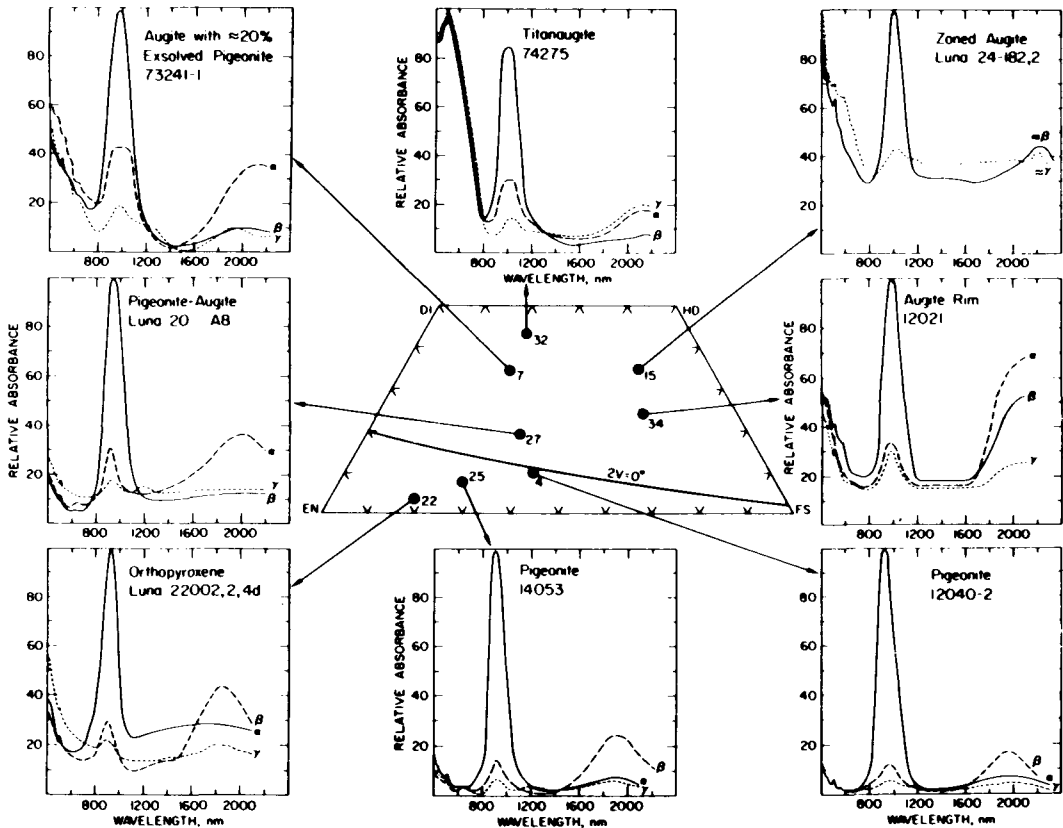


FIG. 2. Polarized absorption spectra of single crystals of pyroxenes in different moon-rock samples (modified from Hazen *et al.*, 1978). Note the intense absorption bands at $\sim 1 \mu\text{m}$ and $\sim 2 \mu\text{m}$ originating from crystal field transitions in pyroxene $\text{Fe}^{2+}/M2$ site cations.

1.25 μm . Pyroxenes, alone, produce a crystal field band in the 2 μm region originating from $\text{Fe}^{2+}/M2$ site cations, the position of which is more diagnostic of pyroxene structure-type than the one micron band (Burns, 1970; Adams, 1974). However, tetrahedrally coordinated Fe^{2+} ions in oxide structures also absorb in the 1.8–1.9 μm region (Bell *et al.*, 1975; Nolet *et al.*, 1979), which can complicate interpretations of pyroxene crystal chemistry (White and Keester, 1966; Bancroft and Burns, 1967) and remote-sensed reflectance spectra of basaltic glass-bearing planetary regoliths (Farr *et al.*, 1980; Dyar and Burns, 1981). Visible-region spectra of pyroxenes contain features attributable to Fe^{3+} , Ti^{3+} , Cr^{3+} , $\text{Fe}^{2+}-\text{Fe}^{3+}$, $\text{Ti}^{3+}-\text{Ti}^{4+}$ and $\text{Fe}^{2+}-\text{Ti}^{4+}$ cation assemblages (Burns and Huggins, 1973; Burns *et al.*, 1973, 1976; Sung *et al.*, 1974; Loeffler *et al.*, 1974, 1975; Rossman, 1980). However, although such spectral features in the 0.4–0.7 μm wavelength range have been used to map Ti-rich mare basalts (Pieters, 1978), mature

lunar regolith (Charette *et al.*, 1974), and Fe^{3+} in bright regions on Mars (Singer, 1985), visible-region spectra are not addressed in this presentation which focuses on Fe^{2+} -bearing mineral and glass assemblages absorbing in the near infrared region.

The spectra illustrated in Figs. 2 and 3 portray compositional-dependencies of the pyroxene absorption bands, which are demonstrated in plots of the 'one micron band' versus the 'two micron band' such as that illustrated in Fig. 4 (Adams, 1974). This pyroxene determinative curve is particularly applicable to powdered samples and has been widely used to interpret remote-sensed reflectance spectra of planetary surfaces. Note, however, that the utility of Fig. 4 depends on the occurrence of Fe^{2+} ions in pyroxene $M2$ sites since crystal field bands for Fe^{2+} ions in pyroxene $M1$ sites, when resolved, occur only in the 1 μm region (Burns, 1970; Rossman, 1980). Therefore, pure enstatite and stoichiometric

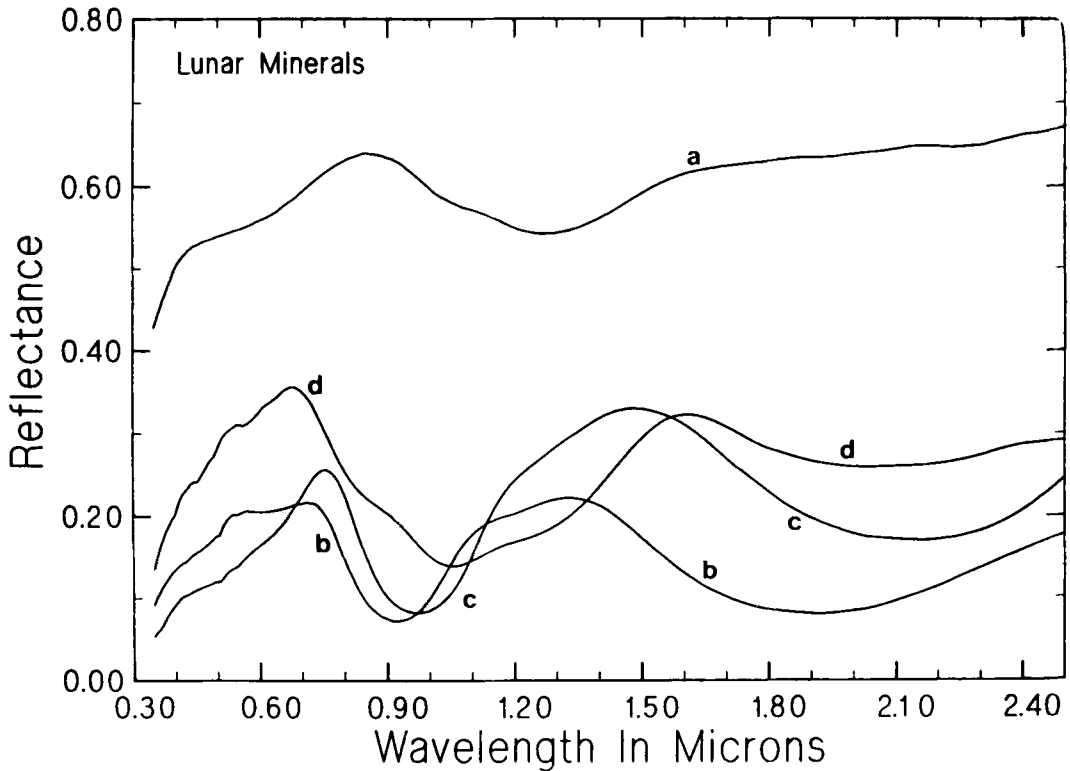


Fig. 3. Diffuse reflectance spectra of powdered lunar minerals containing Fe^{2+} ions: (a) plagioclase feldspar; (b) orthopyroxene; (c) calcic clinopyroxene; and (d) olivine. (Spectra provided by C. M. Pieters).

compositions along the diopside–hedenbergite join cannot be plotted on the $1\ \mu\text{m}$ versus $2\ \mu\text{m}$ curve shown in Fig. 4. Applications of this pyroxene spectral determinative curve are described hereafter.

The Moon: problems of mineral mixtures

The close proximity of the Moon to Earth and its lack of an atmosphere have resulted in the compilation of a large number of telescopic reflectance spectra from diverse areas of the lunar surface (McCord *et al.*, 1981), including mare basalts (Pieters, 1978), pyroclastic mantling deposits (Gaddis *et al.*, 1985) and lunar highlands (Pieters, 1986). Representative examples of such spectra are illustrated in Fig. 5. Absorption features in the $1\ \mu\text{m}$ and $2\ \mu\text{m}$ regions are clearly visible, suggesting that pyroxenes are the dominant minerals at each site. Indeed, correlations with the $1\ \mu\text{m}$ vs. $2\ \mu\text{m}$ determinative curve in Fig. 4 indicate the presence of orthopyroxene in highland soil from Apollo 16 (Fig. 5a), pigeonite

and subcalcic augite in Apollo 17 high-Ti mare basalt (Fig. 5b), and calcic augite in low-Ti basalt from Mare Serenitatis (Fig. 5c) (Gaddis *et al.*, 1985). However, since mono-mineralic assemblages are extremely unlikely on the Moon, the pyroxene-dominated spectra shown in Fig. 5 must have contributions from Fe^{2+} in other phases in the regolith, particularly in the low albedo reflectance spectrum from pyroclastic mantled mare at the Littrow region (Fig. 5d). Mineralogical and optical spectral studies of samples returned from the Moon indicate that pyroxenes coexisting with olivine, plagioclase feldspar, volcanic and impact glasses, and opaque ilmenite and spinels are the most likely phases to modify the pyroxene $1\ \mu\text{m}$ and $2\ \mu\text{m}$ bands. This problem of how one mineral interferes with the spectral features of another has been addressed by reflectance spectral measurements of various mineral mixtures (Nash and Conel, 1974; Singer, 1981; Cloutis *et al.*, 1986; Mustard and Pieters, 1987).

Examples of experimental measurements of mixed-mineral assemblages are illustrated by the

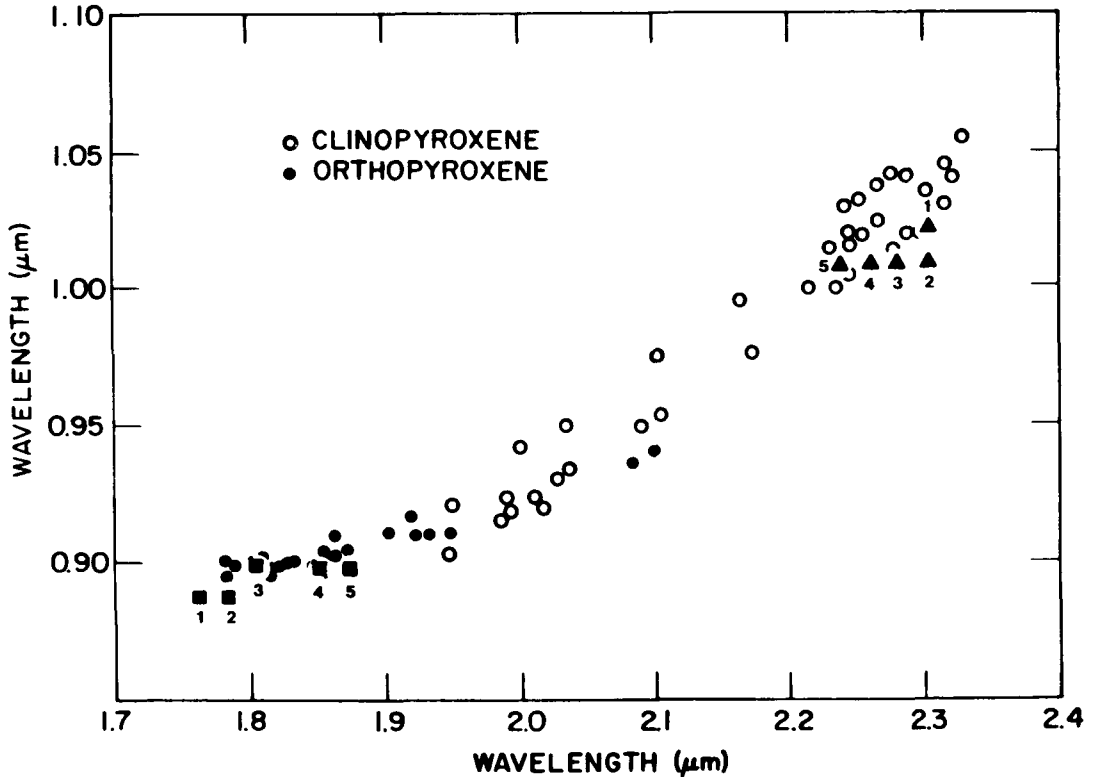


Fig. 4. The $1\ \mu\text{m}$ vs. $2\ \mu\text{m}$ pyroxene spectral determinative curve widely used to identify compositions and structure-types of pyroxene on planetary surfaces (modified from Adams, 1974). Circles refer to room-temperature data. Numbered squares (orthopyroxene $\text{En}_{86}\text{Fs}_{14}$) and triangles (clinopyroxene $\text{Wo}_{42}\text{En}_{51}\text{Fs}_7$) represent spectral data obtained at the temperatures 80 K (1), 173 K (2), 273 K (4) and 448 K (5). (Modified from Singer and Roush, 1985).

spectral data for suites of orthopyroxene-clinopyroxene and orthopyroxene-olivine mixtures in Fig. 6. The gradual shifts of the $1\ \mu\text{m}$ and $2\ \mu\text{m}$ bands are clearly seen for orthopyroxene-clinopyroxene mixtures (Fig. 6a) and, while deleterious broadening of the $1\ \mu\text{m}$ band occurs, the $2\ \mu\text{m}$ band appears to be resolvable into component bands in pyroxene mixtures. The orthopyroxene-olivine mixtures (Fig. 6b) demonstrate that the diagnostic pyroxene $2\ \mu\text{m}$ band is conspicuous even when pyroxene is a minor constituent. However, the characteristic features for olivine at $0.9\ \mu\text{m}$, $1.05\ \mu\text{m}$ and $1.25\ \mu\text{m}$ are quickly obscured by the more intense pyroxene $1\ \mu\text{m}$ band. Fig. 7 showing reflectance spectra of mixtures of orthopyroxene with plagioclase feldspar and magnetite vividly demonstrates how the presence of opaque oxide phases drastically lowers the albedo and intensities of the diagnostic pyroxene absorption features. Metallic

iron in chondritic meteorites is also detrimental to pyroxene spectra (Gaffey, 1976).

Such results for mixed-mineral assemblages enable more elaborate interpretations to be made of the remote reflectance spectra of the Moon shown in Fig. 5 (Gaddis *et al.*, 1985). Olivine and mixed-pyroxene assemblages are responsible for the overall profiles obtained from mare basalts and lunar highlands (Figs. 5a-c). However, band-broadening and low-albedo spectra of dark mantling pyroclastic deposits (Fig. 5d) indicate the presence of volcanic glass which has been partially devitrified to opaque ilmenite-bearing assemblages, such as that those found in Fe-Ti orange glass spherules from Shorty Crater at the Apollo 17 site (Vaughan and Burns, 1973).

The ultimate objective of remote reflectance spectral measurements is to obtain quantitative estimates of the modal mineralogy of unexplored surfaces of the Moon and, indeed, other

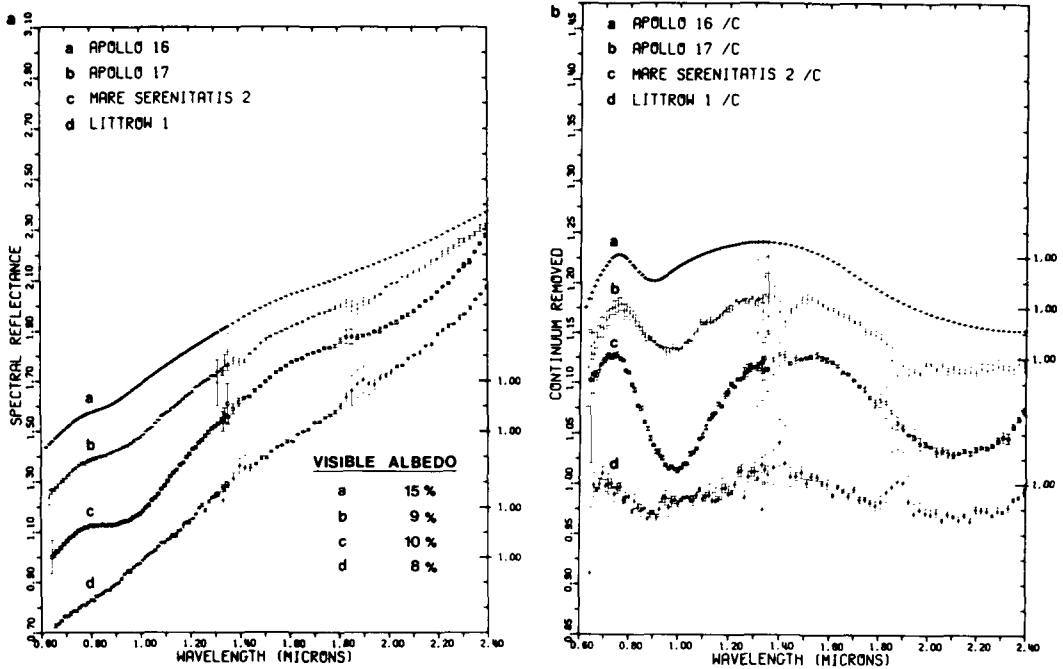


Fig. 5. Remote-sensed spectra of representative areas on the Moon's surface (from Gaddis *et al.*, 1985). Left: telescopic spectral reflectance measurements scaled to unity at $1.02\ \mu\text{m}$ and offset relative to adjacent spectra; Right: residual absorption features for the same measurements after a straight-line continuum through $0.73\ \mu\text{m}$ and $1.6\ \mu\text{m}$ has been removed: (a) highland soil sampled at the Apollo 16 landing site; (b) high-Ti mare basalt at the Apollo 17 landing site; (c) low-Ti mare basalt at Mare Serenitatis; (d) pyroclastic deposits at Taurus-Littrow.

terrestrial planets. This necessitates difficult and elaborate spectrum-curve fitting procedures, which are currently the focus of detailed research (Roush and Singer, 1986; Cloutis *et al.*, 1986; Mustard and Pieters, 1987). Nevertheless, valuable petrological information has been deduced from the reflectance spectral profiles alone. For example, telescopic reflectance spectra for *c.* 5 km diameter areas within the 95 km diameter lunar crater Copernicus shown in Fig. 8 indicate that wall (Fig. 8a) and floor (Fig. 8b) areas with the weak band centered near $0.92\ \mu\text{m}$ diagnostic of orthopyroxenes are typical highland soils of noritic composition and predominate in Copernicus (Pieters *et al.*, 1985). Other floor areas (Fig. 8c) contain high proportions of glass-bearing impact melt. However, central peaks of Copernicus (Fig. 8d) are quite different from the walls and floors. They exhibit a broad multiple band centered near $1.05\ \mu\text{m}$ indicating olivine as the mafic component (Pieters, 1982). Troctolite is thus believed to be the major rock-type forming the central peaks of Copernicus. Reflectance spectra of rays emanating from Copernicus contain more calcic-rich pyr-

roxenes indicative of pigeonite-augite assemblages (Pieters *et al.*, 1985).

Mercury and the Moon: problems of high temperatures

Since reflectance spectra measured through telescopes are produced by sunlight impinging upon the surface of a planet, the effects of temperature on spectral reflectivities of minerals need to be carefully assessed, particularly when large differences exist between extraterrestrial surfaces and ambient conditions on Earth under which calibration measurements have been made. Such situations exist for Mercury ($\sim 650\ \text{K}$), Venus ($\sim 740\ \text{K}$), and the Moon ($\sim 400\ \text{K}$), day-time high temperatures (in parenthesis) of which at their equators are higher than those on Earth. Corresponding sunlit surfaces of Mars ($\sim 280\ \text{K}$) and asteroids ($\sim 175\ \text{K}$), on the other hand, are somewhat lower. Numerous laboratory investigations of temperature-induced changes of mineral spectra have been undertaken, therefore, in order to interpret modal mineralogies of hot and cold

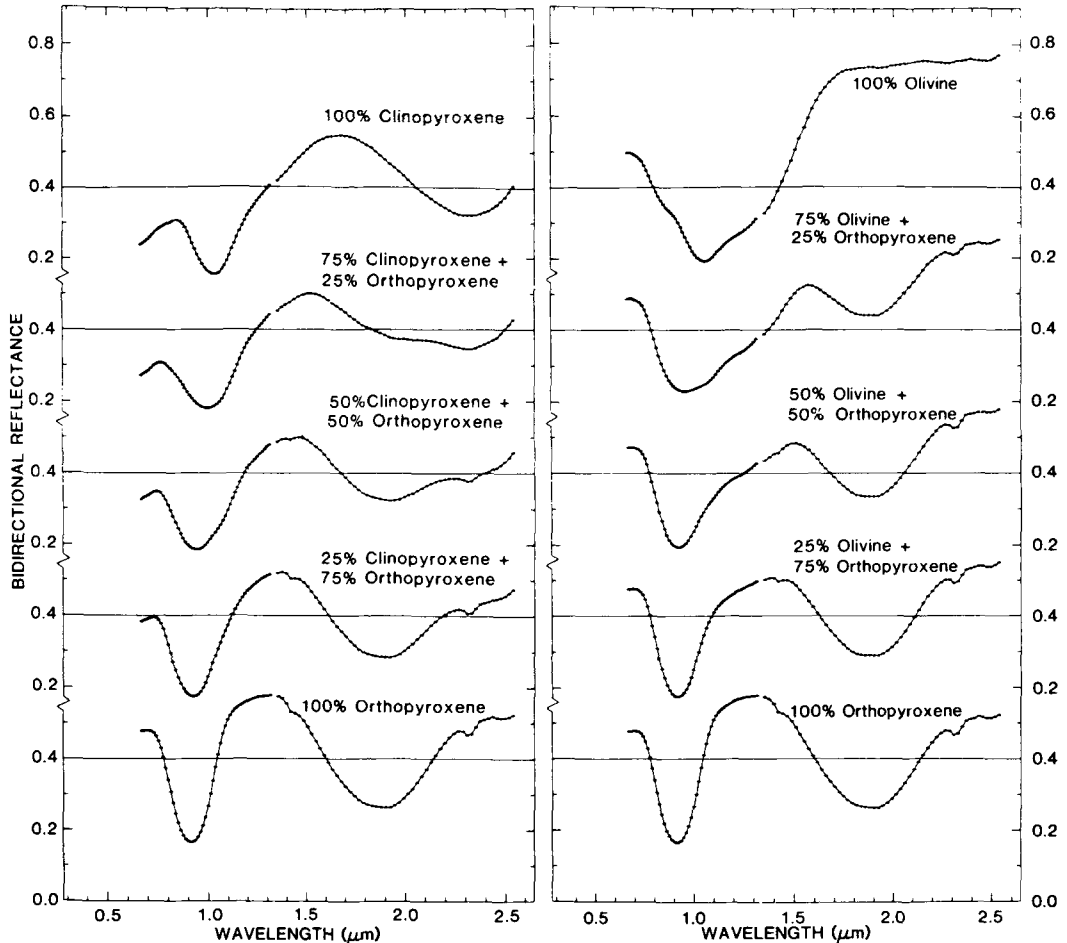


Fig. 6. Reflectance spectra of mixed-mineral assemblages (modified from Singer, 1981). Left: orthopyroxene ($\text{En}_{88}\text{Fs}_{14}$)–clinopyroxene ($\text{Wo}_{41}\text{En}_{51}\text{Fs}_8$) mixtures, in weight percentages; Right: orthopyroxene–olivine ($\text{Fo}_{85}\text{Fa}_{15}$) mixtures. Note how pyroxene dominates the mineral-mixture spectra. Olivine causes broadening of the pyroxene $1\ \mu\text{m}$ band but one olivine feature persists near $1.25\ \mu\text{m}$.

planetary surfaces (Sung *et al.*, 1977; Osborne *et al.*, 1978; Nolet *et al.*, 1979; Parkin and Burns, 1980; Singer and Roush, 1985).

Two important consequences of elevated temperatures on visible–near-infrared spectra are, first, they affect positions and intensities of crystal field bands within a transition metal-bearing mineral and, second, thermal emission by the host mineral, itself, occurs. The effects of temperature on reflectance spectral profiles are elegantly demonstrated by the data for Fe^{2+} in olivine, pyroxenes, and basaltic assemblages shown in Fig. 9. The three components of the olivine spectra centred around $1\ \mu\text{m}$ become better resolved at lower temperatures but show insignificant shifts of band minima (Fig. 9a). However, reflectance

spectra of pyroxenes (Figs. 9b and c) show dramatic changes of band shape with rising temperature, particularly at the longer wavelength edges. In common with olivines, the pyroxene $1\ \mu\text{m}$ bands also show only minor wavelength shifts. However, in marked contrast to the $1\ \mu\text{m}$ bands, the pyroxene $2\ \mu\text{m}$ bands show major differences of temperature-induced shifts; for orthopyroxenes, this band increases from $\sim 1.80\ \mu\text{m}$ to $\sim 1.90\ \mu\text{m}$ between 80 K and 448 K (Fig. 9b), whereas for clinopyroxenes it decreases from $\sim 2.35\ \mu\text{m}$ to $\sim 2.25\ \mu\text{m}$ over the same temperature range (Fig. 9c). As a result, two pyroxenes are clearly resolvable in basaltic assemblages at low temperatures (Fig. 9d). However, such resolution of individual pyroxene bands is not achiev-

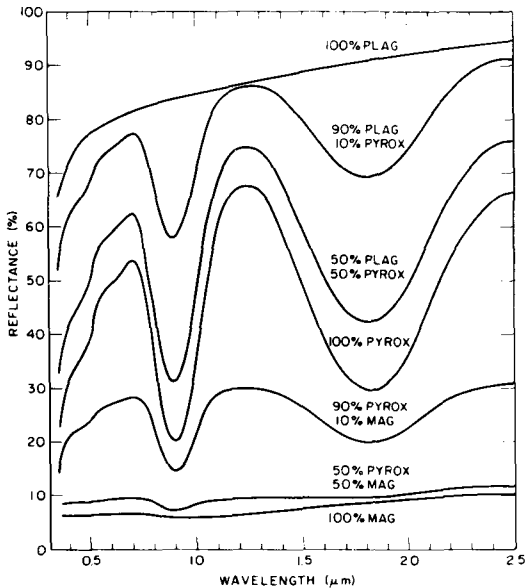


Fig. 7. Diffuse reflectance spectra of mixtures of orthopyroxene with plagioclase feldspar and magnetite (from Adams, 1974, attributed to C. M. Pieters). Note how the opaque oxide phase swamps the diagnostic pyroxene bands at $1\ \mu\text{m}$ and $2\ \mu\text{m}$.

able at the higher temperatures applicable to sunlit surfaces of the Moon (*c.* 400 K). Thus, broadband features in the $2\ \mu\text{m}$ region observed in lunar remote-sensed reflectance spectra (Figs. 5 and 8) are suggestive of two-pyroxene assemblages and, perhaps, contributions from tetrahedral Fe^{2+} in basaltic glass (Farr *et al.*, 1980; Dyar and Burns, 1981).

The contrasting temperature-induced shifts of the pyroxene $1\ \mu\text{m}$ and $2\ \mu\text{m}$ bands may lead to erroneous estimates of the composition, and to a lesser extent structure-type, of a pyroxene-bearing mineral assemblage deduced from the remote-sensed reflectance spectrum of a hot or cold planetary surface if room-temperature determinative curves, such as that shown in Fig. 4, are used uncritically. For example, remote-sensed spectra of hot-planet surfaces such as those on the Moon would lead to overestimates of Fe^{2+} contents of its orthopyroxenes and underestimated Fe^{2+} contents of the clinopyroxene (Singer and Roush, 1985). Cold-surface planets such as Mars and asteroids could produce opposite results. On the other hand, the room-temperature data underlying the pyroxene determinative curve shown in Fig. 4 may impose constraints on the compositions of pyroxenes deduced from telescopic spectra of

a planet with very high surface temperatures, such as Mercury.

The hot surface of Mercury, as well as reflecting sunlight, also behaves as a quasi-blackbody radiator and emits thermal energy back into space, too. As a result, the spectral reflectance of Mercury rises sharply above $\sim 1.5\ \mu\text{m}$ due to its thermal emissivity obscuring any possible contribution from a Fe^{2+} -pyroxene $2\ \mu\text{m}$ band. The close proximity of Mercury to the Sun makes telescopic reflectance spectral measurements of its surface very difficult, so that attempts to identify pyroxenes on Mercury and to estimate their compositions from the $1\ \mu\text{m}$ band alone have produced ambiguous results. For example, a weak broad band resolved at $0.89\ \mu\text{m}$ (McCord and Clark, 1979) and corresponding to the lowest limit for an orthopyroxene in the room-temperature pyroxene determinative curve shown in Fig. 5 might imply the presence of enstatite in low-iron basalts on the surface of Mercury. However, temperature-induced variations of the orthopyroxene $1\ \mu\text{m}$ band, such as those portrayed in Fig. 9a showing that Fe^{2+} contents of orthopyroxenes are overestimated from high-temperature spectra, suggest that the $0.89\ \mu\text{m}$ feature is impossibly low to be assigned to Fe^{2+} in orthopyroxene on Mercury. Pure end-member enstatite or diopside could occur on Mercury, but these pyroxenes would not be identified by spectral reflectance. The $0.89\ \mu\text{m}$ band could be indicative of ferric-bearing augites (Burns *et al.*, 1976) in the regolith of Mercury since Fe^{3+} crystal field transitions intensify considerably but do not shift much at elevated temperatures (Parkin and Burns, 1980).

Venus and Mars: problems of atmospheres and oxidative weathering

The surface of the Moon and Mercury are conducive to telescopic spectral measurements, albeit complicated by effects of high temperatures, because they lack atmospheres. The presence of atmospheric gases on Venus and Mars impose severe problems on the measurement and interpretation of earth-based remote-sensed reflectance spectra obtained from these planets. The problem is most acute for Venus because its hot surface is masked by the dense atmosphere which strongly absorbs and scatters visible-near-infrared radiation. However, Soviet Venera missions to the Venusian surface have yielded spectrophotometric data in the form of multispectral images at three wavelengths in the visible region ($0.44\ \mu\text{m}$, $0.54\ \mu\text{m}$, and $0.63\ \mu\text{m}$) from which surface mineralogy has been deduced (Pieters *et al.*, 1986). After correcting for effects of orange-

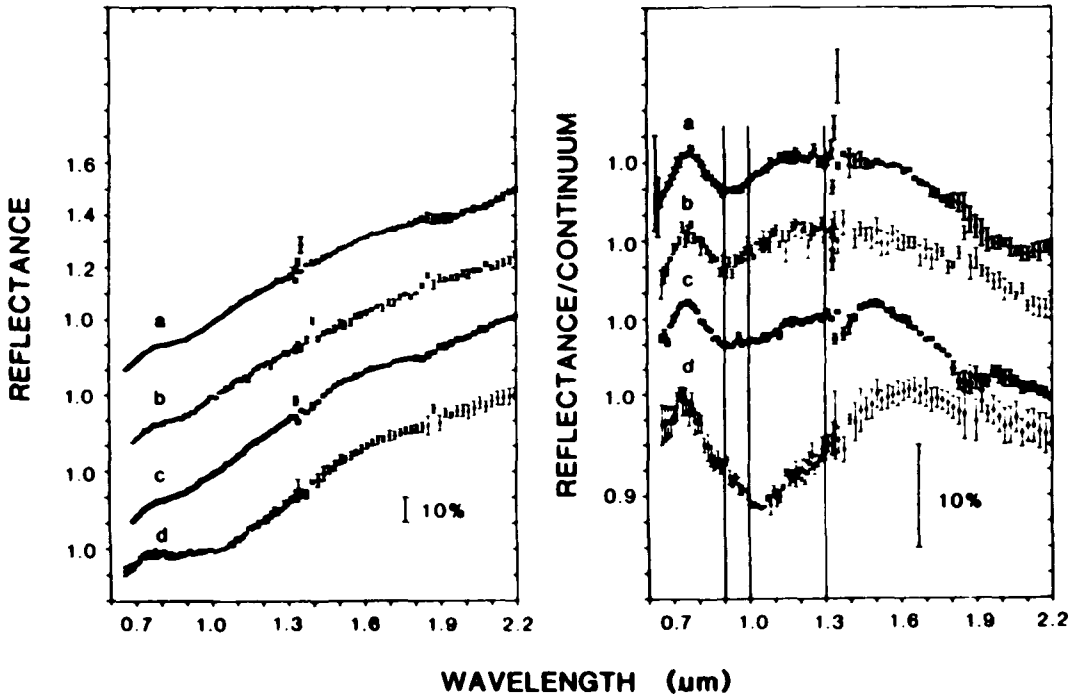


Fig. 8. Reflectance spectra obtained from Earth-based telescopes for small (<5 km diameter) areas within the Copernicus crater on the Moon (from Pieters *et al.*, 1986). Left: reflectances scaled to unity at 1.02 μm ; Right: residual absorption after continuum removal. Spectra are offset vertically. (a) Wall and (b) floor areas containing orthopyroxene are deduced to be of noritic composition; (c) floor containing pyroxene and glass is an area of extensive impact melt; (d) central peak containing olivine is deduced to be troctolite.

colouration due to the atmosphere, the surface of Venus appears to be dark without significant colour. Correlations with high-temperature laboratory reflectance spectra of oxidized basaltic materials suggest that the basaltic surface of Venus contains ferric-bearing minerals, possibly formed from oxidation of pyroxenes and olivine (Pieters *et al.*, 1986).

The surface of Mars, on the other hand, is visible and has been accessible to several Earth-based telescopic reflectance spectral measurements in the visible and infrared regions, as well as *in situ* multispectral images of the surface taken during the Viking orbiter and lander experiments (Singer, 1985). However, while thermal emissivity of the relatively cold surface of Mars becomes dominant only beyond the 5 μm wavelength region, the presence of atmospheric CO_2 and traces of H_2O mask critical regions in the near-infrared spectra needed for positive identification of ferromagnesian silicates in the martian regolith. To a close approximation, Mars' surface is composed of bimodal high- and low-albedo regions (Singer, 1985) which give rise to the typi-

cal bright-region and dark-region spectra illustrated in Fig. 10. Bright-region spectra are dominated by spectral features, including the broad band at $\sim 0.87 \mu\text{m}$, attributed to crystal field transitions in Fe^{3+} ions; atmospheric CO_2 is responsible for the sharper features at 1.45 μm , 1.62 μm , and 1.9–2.1 μm . The Fe^{3+} spectral features lack specificity and a variety of ferric-bearing phases have been suggested as oxidative weathering products on Mars' surface, including poorly crystalline oxides, clay silicate and sulphate phases (Sherman *et al.*, 1982; Singer, 1985; Burns, 1986). Of greater interest, so far as this presentation is concerned, are the dark-region spectra in which Fe^{3+} ions, although present, do not obscure contributions from Fe^{2+} ions in the 1 μm region. These spectral features indicate the presence of pyroxenes and, perhaps olivine in iron-rich basalts believed to underlie Mars' surface. Unfortunately, interference by atmospheric CO_2 at 1.9–2.1 μm makes it extremely difficult, if not impossible, to identify the pyroxene structure-type and composition from its diagnostic 2 μm band. However, the presence of pigeonite-augite

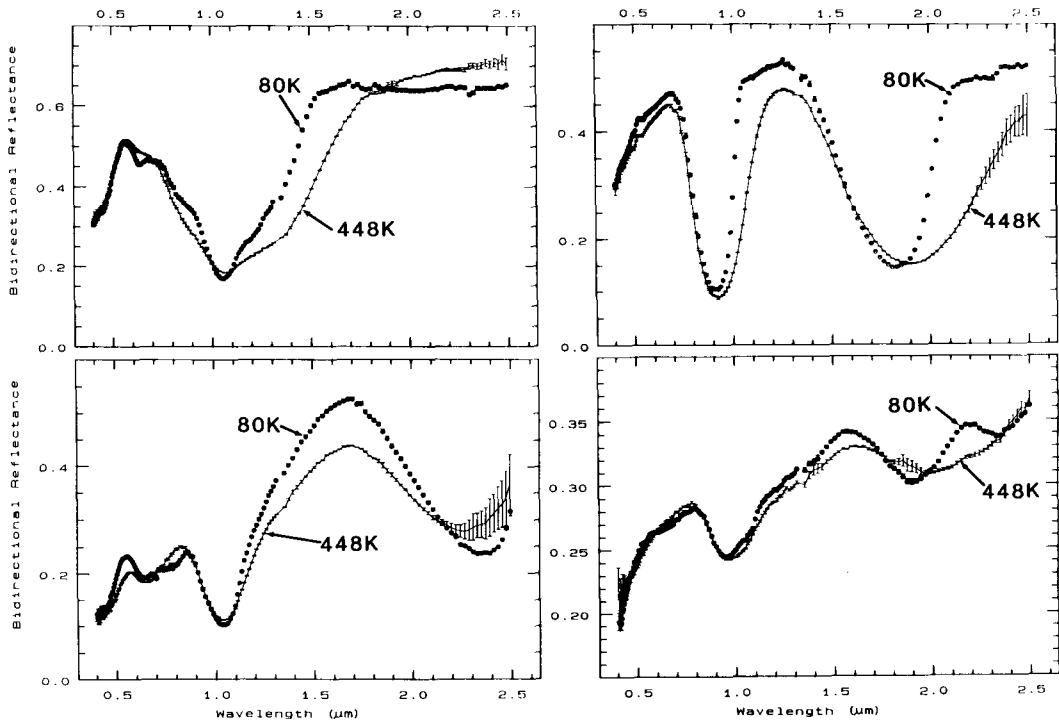


FIG. 9. Temperature variations of reflectance spectra of Fe^{2+} -bearing silicate mineral and basaltic assemblages (adapted from Singer and Roush, 1985). Top left: olivine, $\text{Fo}_{89}\text{Fa}_{11}$; Top right: bronzite, $\text{En}_{86}\text{Fs}_{14}$; Bottom left: augite, $\text{Wo}_{42}\text{En}_{51}\text{Fs}_7$; Bottom right: basaltic assemblage, comprising orthopyroxene, pigeonite-augite intergrowth, olivine and plagioclase feldspar. Note that the temperature variations of the $1\ \mu\text{m}$ and $2\ \mu\text{m}$ bands for the two pyroxenes are plotted on Fig. 4.

(\pm olivine) assemblages in meteoritic shergottites believed to have originated from Mars are consistent with the broad spectral features at $1\ \mu\text{m}$ and, perhaps underlying the CO_2 absorption bands at $c. 2\ \mu\text{m}$.

Correlations with meteorite spectra

Before the advent of the Apollo and Luna missions which retrieved samples from the Moon's surface, meteorites provided the only source of extraterrestrial materials and raised questions about their sources from parent bodies such as asteroids. Visible-near-infrared reflectance spectroscopy, therefore, has been applied extensively to laboratory investigations of meteorites and to remote-sensed measurements of many asteroids (Gaffey, 1976; Gaffey and McCord, 1978; McFadden *et al.*, 1982, 1984; Bell and Keil, 1988).

Spectral reflectance curves for the range of meteorite types are illustrated in Fig. 11. These spectra demonstrate the diagnostic features of the various meteorite types, including the presence

or absence of absorption bands, their positions and relative intensities, their symmetries and widths, and other properties such as continuum slope, curvature, and inflexion points (Gaffey, 1976). Again, noteworthy features of the meteorite spectra are the prominent pyroxene $1\ \mu\text{m}$ and $2\ \mu\text{m}$ bands, the relative intensities and asymmetries of which have been used to characterize the pyroxenes and to estimate olivine/pyroxene ratios in meteorites. Relating these meteorite spectra to those of asteroids has been difficult due to the faintness of these objects in space. Nevertheless, recent telescopic spectra measurements have led to discoveries of several large asteroids containing olivine-rich dunite-like rocks (Cruikshank and Hartmann, 1984), as well as other asteroids with wide ranges of olivine/pyroxene ratios, which are inconsistent with an ordinary-chondritic composition but suggestive of affinities with stony-iron meteorites (Bell and Keil, 1988). The spectra of other asteroids, including 4 Vesta and 1915 Quetzalcoatl, resemble basaltic achondrites (McFadden *et al.*, 1982) suggesting that they

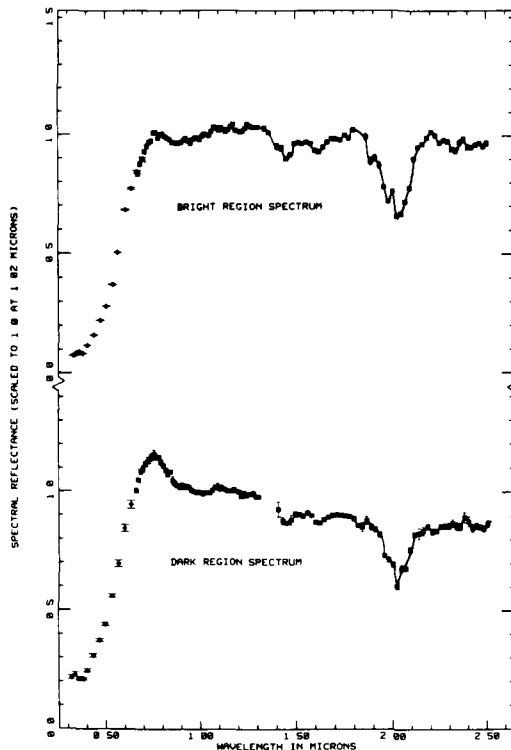


Fig. 10. Representative bright and dark region reflectance spectra of Mars obtained through earth-based telescopes and scaled to unity at $1.02\ \mu\text{m}$ (from Singer *et al.*, 1979). The band near $0.87\ \mu\text{m}$ in bright-region spectra is assigned to Fe^{3+} . Pyroxenes and, perhaps, olivine, contribute to the broad band at $0.9\text{--}1.1\ \mu\text{m}$ in dark-region spectra. The $2\ \mu\text{m}$ pyroxene $\text{Fe}^{2+}/M2$ site band is obscured by CO_2 in the atmosphere of Mars. CO_2 is also responsible for the peaks at $\sim 1.4\ \mu\text{m}$ and $1.62\ \mu\text{m}$.

underwent internal heating and differentiation. Thus, asteroids like Vesta and Quetzalcoatl are very likely sources of the large and varied meteorites of the eucrite, howardite, and diogenite groups.

Meteorites collected from Antarctica in the past decade have yielded unique specimens which appear to have originated from the terrestrial planets themselves. They include three meteorites with lunar affinities and two shergottites belonging to the SNC group of nine meteorites believed to have originated from Mars. One of the lunar meteorites (ALHA 81005) is a regolith breccia analogous to rock-types found in the lunar highlands. A composite diffuse reflectance spectrum of this meteorite shows a band centred near $0.98\ \mu\text{m}$ indicative of subcalcic augite, together with features attributed to olivine and Fe^{2+} -bear-

ing plagioclase feldspars (Pieters *et al.*, 1983). However, this spectrum profile does not match telescopic reflectance spectra obtained from ~ 150 small areas $3\text{--}20\ \text{km}$ in diameter on the Moon's surface, including young highland craters. The spectral data suggest that this lunar meteorite is derived from a surface unit on the Moon not previously sampled, and that the most probable source area is the near-side limb or the far side of the Moon. The Antarctic shergottite EETA 79001, with impact-glass pockets containing trapped gases resembling the composition of the martian atmosphere, contains calcite, gypsum and sulphur-rich aluminosilicate phases which were suggested to be relict grains of chemical weathering products on Mars (Gooding and Muenow, 1986; Gooding *et al.*, 1988). However, negligible ferric iron was resolved in Mössbauer spectral measurements of the impact glasses, while the pyroxene-dominated matrix of EETA 79001 contains less than 2 wt.% Fe^{3+} (Solberg and Burns, 1988), conforming with evidence from diffuse reflectance spectra of other SNC meteorites which failed to detect ferric iron and suggesting that these meteorites did not originate from the outermost surface of Mars.

Summary and future directions

Reflectance spectroscopy has proven to be the most powerful and versatile remote-sensing technique for determining surface mineralogy, chemical compositions and lithologies of planetary objects, as well as constituents of their atmospheres. Table 1 summarizes information that has been deduced for the terrestrial planets based on spectral properties of light in the visible and near infrared regions reflected from their surfaces.

The planetary reflectance spectral data constituting Table 1 traditionally have been obtained with Earth-based telescopes. Such remote-sensed measurements are limited by telescope availability, favourable observational conditions, and optimum viewing alignments of the planetary objects. As a result, comparatively few high-quality telescopic spectra (perhaps numbering several hundreds) are available for the solar system planets and their satellites. However, this situation is about to change dramatically.

Future spacecraft missions to solar system objects are primarily being oriented towards remote-sensing experiments, in contrast to the soft-landed *in situ* experiments and sample return initiatives during the 1970s. Because reflectance spectroscopy has become one of the most important investigative techniques in the planetary sciences, current and planned space missions for the

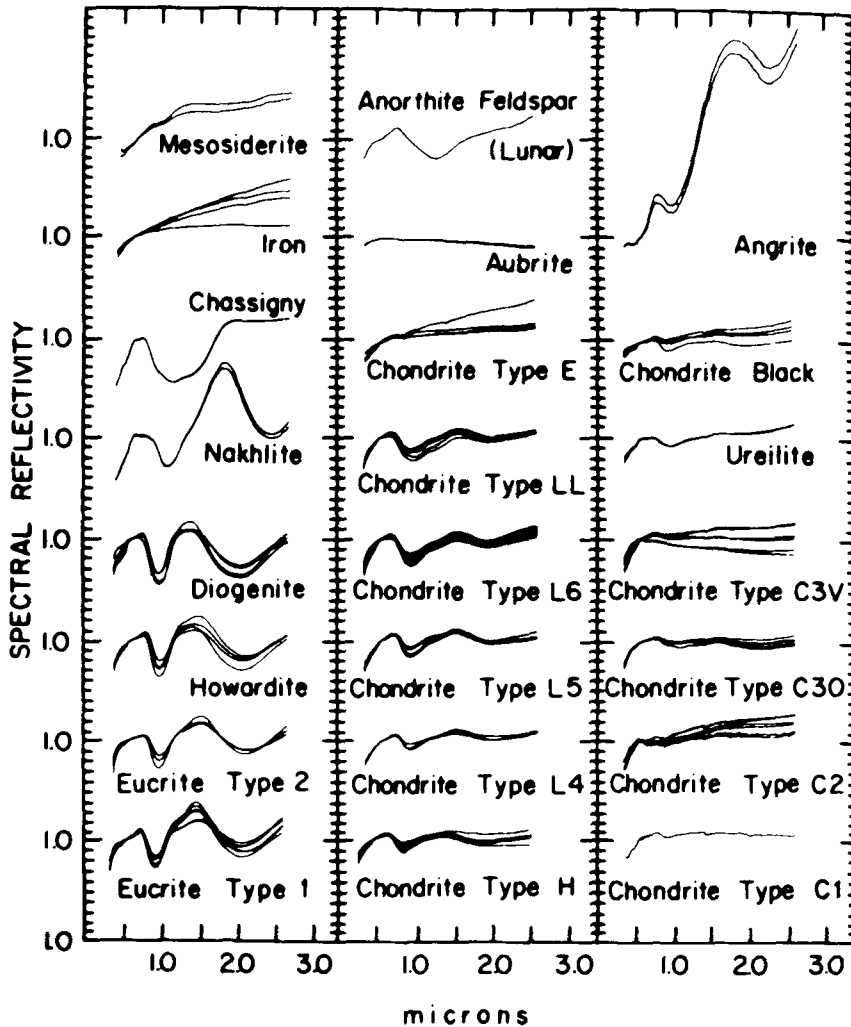


Fig. 11. Normalized spectral reflectance curves for the range of meteorite types (from Gaffey, 1976).

1990s will include visible and near infrared spectrometers in their instrument payloads. Examples include: the *Galileo Orbiter/Probe* mission to Jupiter; the *Mars Orbiter* mission to Phobos; the *Comet Rendezvous Asteroid Flyby (CRAF)* mission, which will match orbits with a comet and study an asteroid en route; the *Cassini* mission to Saturn, which will send a probe to Titan's surface; the *Lunar Geoscience Observer* mission to study ancient cratering and volcanism on the Moon; and, perhaps the most ambitious project this century, the *Mars Rover/Sample Return* mission. Reflectance spectral measurements from space will provide more favourable viewing geometries, eliminate problems due to telluric water

and CO_2 , and improve the resolution of areas scanned on a nearby planetary surface.

However, these future spacecraft missions will produce a flood of spectroscopic data unprecedented in solar system exploration. There is now a challenge to develop high-speed data processing systems to analyse and interpret, on a real-time basis, vast arrays of reflectance spectra during their rapid transmission back to Earth.

To keep abreast of this future mass of remote-sensed data, laboratory experiments and theoretical models need to be developed to provide background information for interpreting the on-line spacecraft reflectance spectral data from planetary surfaces. Studies of a qualitative nature

Table 1. Surface Constituents of Terrestrial Planets Deduced from Remote-Sensed Spectroscopy

Planet	Equatorial Diameter (km)	Mean Distance from Earth (10 ⁸ km)	Temperature (K)	Atmospheric Pressure (atmos.)	Surface Mineralogy and Petrology ^b
Earth	12756	-	315	1	Igneous, sedimentary and metamorphic rocks.
Mercury	4878	91.7	650	-	Lunar-like surface but with lower Fe ²⁺ content; traces of atmospheric Na implies sputtering from Na-bearing minerals.
Venus	12104	41.4	740	96	Oxidized basaltic surface; CO ₂ dominated atmosphere with some CO, HCl, HF and SO ₂ ; H ₂ SO ₄ in clouds.
Moon	3476	0.384	400	-	Mare basalts contain olivine, Fe ²⁺ -bearing plagioclase and basaltic glasses, Fe ²⁺ -Ti ³⁺ -bearing pyroxenes and glasses, and abundant opaque phases; highland anorthosites contain shocked and unshocked plagioclases; vitrification (agglutinates) by impact events; solar wind darkening; existence of many lithologic units unsampled by Apollo and Luna missions; olivine-rich rocks (troctolites) in central peaks of craters.
Mars	6796	78.3	280	0.01	Mafic silicates in dark regions, pyroxenes detected locally, olivine suspected; Fe ³⁺ phases in bright regions and clay minerals in global dust are oxidative weathering products; H ₂ O (frost) condensates; ice at north pole, "dry ice" (CO ₂) at south pole.
Asteroids					
Vesta	540	204	180		Fe ²⁺ -bearing pyroxenes, olivine and plagioclase; some asteroids have fine-grained regolith; impact-produced glasses are rare; at least 14 asteroid spectral classes exist; close resemblance between some asteroid and meteorite spectra suggest parent asteroid bodies; Vesta and basaltic achondrites indicate a differentiated parent body.
Pallas	610	264	175		
Ceres	1020	264	175		

^a maximum day-time high temperature at the equator

^b based on McCord (1988)

described earlier in this presentation have demonstrated that spectral reflectance profiles of planetary surface materials are influenced primarily by the chemical compositions and abundances of constituent minerals. There is now an increasing awareness of second-order effects, such as temperature, viewing geometry, grain size and particle packing, on positions and intensities of diagnostic mineral spectral features. Research is needed to quantify these effects and to more closely simulate physical properties of planetary regoliths when they reflect sunlight. Such projects include spectral measurements for mineral assemblages having different temperatures, particle sizes, grain-size packings, and modal mineral proportions, over a range of angles of incident and reflected light and in confining atmospheres having a variety of pressures and compositions. Other effects such as atmospheric weathering and radiation sputtering processes under different intensities and exposure times also need to be assessed. The ultimate goal of such laboratory investigations is to develop a theoretical model for deducing the modal mineralogy of an area on a planetary surface from its reflectance spectrum measured under known lighting conditions.

Exciting times lie ahead for mineral spectroscopists. As the intensity of effort increases, broadened by the range of problems that can be addressed by the diversity of spectroscopic methods now becoming available, the probability increases that more and more mineralogists will

see the light and become focussed on heaven-sent opportunities to investigate solar system objects remotely by measuring their spectral characteristics.

Acknowledgments

This presentation is dedicated to the team of graduate student and colleague investigators with whom I have collaborated in spectral mineralogy research for the past 20 years. They include: Rateb Abu-Eid, Kris Anderson, Mike Bancroft, Karen Bartels, Jim Besancon, Mike Charette, Mike Clark, Roger Clark, Darby Dyar, Duncan Fisher, Susan Flamm, Mike Gaffey, Colin Greaves, Bob Hazen, Frank Huggins, Bob Huguenin, Tony Law, Irene Leung, Bruce Loeffler, Catherine McCammon, Lucy McFadden, Anne Morawsky, Dan Nolet, Margery Osborne, Kay Parkin, Carle Pieters, Jean Prentice, Virginia Ryan, Martha Schaefer, Ken Schwartz, Dave Sherman, Bob Singer, Teresa Soldberg, D'Arcy Straub, Chien-Min Sung, Matthew Tew, Jack Tossell, David Vaughan, Earle Whipple, Martlee Witner and Valerie Wood. Over the years, Virginia Mee Burns has been extremely supportive. Stimulating discussions have taken place with John Adams, Mike Bancroft, Peter Bell, Keith Johnson, David Mao, Tom McCord, George Rossman, Bill White and, in particular, Carle Pieters, Bob Singer and David Vaughan. Thanks are due to Carle Pieters and Bob Singer who provided many of the spectra used in this presentation. The research was supported throughout by grants from the National Aeronautics and Space Administration (grant numbers: NGR 22-009-551 and 187; NSG 7604; and NAGW-1078).

References

- Abu-Eid, R. M. (1976) Absorption spectra of transition metal-bearing minerals at high pressures. In *The Physics and Chemistry of Minerals and Rocks* (R. G. J. Strens, ed.) J. Wiley, New York, 641–75.
- Adams, J. B. (1968) Lunar and martian surfaces: petrologic significance of absorption bands in the near infrared. *Science* **159**, 1453–5.
- (1974) Visible and near-infrared diffuse reflectance: spectra of pyroxenes as applied to remote sensing of solid objects in the solar system. *J. Geophys. Res.* **79**, 4829–36.
- (1975) Interpretations of visible and near-infrared diffuse reflectance spectra of pyroxenes and other rock-forming minerals. In *Infrared and Raman Spectroscopy of Lunar and Terrestrial Minerals*. (C. Karr, Jr., ed.) Academic Press, New York, 91–116.
- Bancroft, G. M. and Burns, R. G. (1967) Interpretation of the electronic spectra of iron in pyroxenes. *Am. Mineral.* **52**, 1278–87.
- Bell, J. F. and Keil, K. (1988) Spectral alteration effects in chondritic gas-rich breccias: implications for S-class and Q-class asteroids. *Proc. Lunar Planet. Sci. Conf.*, **19th**, 573–80. (Cambridge Univ. Press)
- Bell, P. M., Mao, H. K. and Rossman, G. R. (1975) Absorption spectroscopy of ionic and molecular units in crystals and glasses. In *Infrared and Raman Spectroscopy of Lunar and Terrestrial Minerals*. (C. Karr, Jr., ed.) Academic Press, New York, 1–38.
- Burns, R. G. (1965) *Electronic spectra of silicate minerals: applications of crystal field theory to aspects of geochemistry*. PhD. Diss., Univ. Calif. Berkeley, California.
- (1966a) Origin of optical pleochroism in orthopyroxenes. *Mineral. Mag.* **35**, 715–9.
- (1966b) Apparatus for measuring polarized absorption spectra of small crystals. *J. Sci. Instruments* **43**, 58–60.
- (1970) *Mineralogical Applications of Crystal Field Theory*. Cambridge Univ. Press, London.
- (1974) The polarized spectra of iron in silicates: olivine. A discussion of neglected contributions from Fe²⁺ ions in M(1) sites. *Am. Mineral.* **59**, 625–9.
- (1982) Electronic spectra of minerals at high pressures: How the mantle excites electrons. In *High-Pressure Researches in Geoscience* (W. Schreyer, ed.) E. Schweizerbart'sche Verlagsbuchhandlung, Stuttgart, 223–46.
- (1985) Thermodynamic data from crystal field spectra. In *Microscopic to Macroscopic: Atomic Environments to Mineral Thermodynamics*. (S. W. Kieffer and A. Navrotsky, eds.) *Rev. Mineral.* **14**, 277–316.
- (1986) Terrestrial analogues of the surface rocks on Mars. *Nature* **320**, 55–6.
- and Huggins, F. A. (1973) Visible-region absorption spectra of a Ti³⁺ fassaite from the Allende meteorite: a discussion. *Am. Mineral.* **58**, 955–61.
- and Vaughan, D. J. (1975) Polarized electronic spectra. In *Infrared and Raman Spectroscopy of Lunar and Terrestrial Minerals*. (C. Karr, Jr., ed.) Academic Press, New York, 39–76.
- Abu-Eid, R. M. and Huggins, F. E. (1972a) Crystal field spectra of lunar pyroxenes. *Proc. Lunar Sci. Conf.*, **3rd** **1**, 533–43.
- Huggins, F. E., and Abu-Eid, R. M. (1972b) Polarized absorption spectra of single crystals of lunar pyroxenes and olivines. *Moon* **4**, 93–102.
- Vaughan, D. J., Abu-Eid, R. M., Witner, M. and Morawsky, A. (1973) Spectral evidence for Cr³⁺, Ti³⁺, and Fe²⁺ rather than Cr²⁺ and Fe²⁺ in lunar ferromagnesian silicates. *Proc. Lunar Sci. Conf.*, **4th**, 983–94.
- Parkin, K. M., Loeffler, B. M., Leung, I. S. and Abu-Eid, R. M. (1976) Further characteristics of spectral features attributable to titanium on the moon. *Ibid.* **7th**, 2561–78.
- Charette, M. P., McCord, T. B., Pieters, C. and Adams, J. B. (1974) Application of remote spectral reflectance measurements to lunar geology classification and determination of titanium content of lunar soils. *J. Geophys. Res.* **79**, 1605–13.
- Cloutis, E. A., Gaffey, M. J., Jackowski, T. L. and Reed, K. L. (1986) Calibrations of phase abundance, composition, and particle size distribution for olivine-orthopyroxene mixtures from reflectance spectra. *Ibid.* **91**, 11641–53.
- Cruikshank, D. P. and Hartmann, W. K. (1984) The meteorite-asteroid connection: Two olivine-rich asteroids. *Science* **223**, 281–2.
- Dyar, M. D., and Burns, R. G. (1981) Coordination chemistry of iron in glasses contributing to remote-sensed spectra of the moon. *Proc. Lunar Planet. Sci. Conf.*, **12th**, 695–702.
- Farr, T. G., Bates, B. A., Ralph, R. L. and Adams, J. B. (1980) Effects of overlapping optical absorption bands of pyroxene and glass on the reflectance spectra of lunar soils. *Ibid.* **11th**, 719–29.
- Gaddis, L. R., Pieters, C. M. and Hawke, B. R. (1985) Remote sensing of lunar pyroclastic mantling deposits. *Icarus* **61**, 461–89.
- Garrey, M. J. (1976) Spectral reflectance characteristics of the meteorite classes. *J. Geophys. Res.* **81**, 905–20.
- and McCord, T. B. (1978) Asteroid surface materials: mineralogical characterization from reflectance spectroscopy. *Space Sci. Rev.* **21**, 555–628.
- Goldman, D. S. and Rossman, G. W. (1977) The spectra of iron in orthopyroxenes revisited: the splitting of the ground state. *Am. Mineral.* **62**, 151–7.
- Gooding, J. L. and Muenow, D. W. (1986) Martian volatiles in shergottite EETA 79001: new evidence from oxidized sulfur and sulfur-rich aluminosilicates. *Geochim. Cosmochim. Acta* **50**, 1049–59.
- Wentworth, S. J. and Zolensky, M. E. (1988) Calcium carbonate and sulfate of possible extraterrestrial origin in the EETA 79001 meteorite. *Ibid.* **52**, 909–15.
- Hallimond, A. F. (1956) *Manual of the Polarizing Microscope*. Cooke, Troughton, and Simms; York.
- Hazen, R. M., Mao, H. K. and Bell, P. M. (1977) Effects of compositional variation on absorption spectra of lunar olivines. *Proc. Lunar Sci. Conf.*, **8th**, 1081–90.
- Bell, P. M. and Mao, H. K. (1978) Effects of compositional variation on absorption spectra of lunar pyroxenes. *Ibid.* **9th**, 2919–34.

- Loeffler, B. M., Burns, R. G., Tossell, J. A., Vaughan, D. J. and Johnson, K. H. (1974) Charge transfer in lunar materials: interpretations of ultraviolet-visible spectral properties of the moon. *Ibid.* **5th**, 3, 3007-16.
- (1975) Metal-metal charge transfer transitions: interpretation of visible-region spectra of the moon and lunar materials. *Ibid.* **6th**, 2663-76.
- McCord, T. B. and Adams, J. B. (1969) Spectral reflectivity of Mars. *Science* **163**, 1058-60.
- and Clark, R. N. (1979) The Mercury soil: presence of Fe²⁺. *J. Geophys. Res.* **84**, 7664-8.
- Hawke, B. R., McFadden, L. A., Owensby, P. H., Pieters, C. M. and Adams, J. B. (1981) Moon: near-infrared spectral reflectance, a first good look. *Ibid.* **86**, 10883-92.
- McCord, T. M., ed. (1988) *Reflectance Spectroscopy in Planetary Science: Review and Strategy for the Future*. NASA Spec. Rept. 493, Planet. Geol. Geophys. Progr., 37pp.
- McFadden, L. A., Gaffey, M. J., Takeda, H., Jackowski, T. L. and Reed, K. L. (1982) Reflectance spectroscopy of diogenite meteorite types from Antarctica and their relationship to asteroids. *Mem. Nat. Inst. Plar Res.* **25**, 188-206.
- and McCord, T. B. (1984) Mineralogical-petrological characterization of near-Earth asteroids. *Icarus* **59**, 25-40.
- Mao, H. K. and Bell, P. M. (1973) Polarized crystal field spectra of the moon. In *Analytical Methods Developed for Application to Lunar-Sample Analysis*. Amer. Soc. Testing Materials, STP 539, 100-19.
- Mustard, J. F. and Pieters, C. M. (1987) Quantitative abundance estimates from bidirectional reflectance measurements. *J. Geophys. Res.* **92**, E617-26.
- Nash, D. B. and Conel, J. E. (1974) Spectral reflectance systematics for mixtures of powdered hypersthene, labradorite, and ilmenite. *Ibid.* **79**, 1615-21.
- Nolet, D. A., Burns, R. G., Flamm, S. L. and Besancon, J. R. (1979) Spectra of Fe-Ti silicate glasses: implications to remote-sensing of planetary surfaces. *Proc. Lunar Planet. Sci.*, **10th**, 1775-86.
- Osborne, M. D., Parkin, K. M. and Burns, R. G. (1978) Temperature-dependence of Fe-Ti spectra in the visible region: implications to mapping Ti concentrations on hot planetary surface. *Ibid.* **9th**, 2949-60.
- Parkin, K. M. and Burns, R. G. (1980) High-temperature crystal field spectra of transition metal-bearing minerals: relevance to remote-sensed spectra of planetary surfaces. *Ibid.* **11th**, 731-55.
- Pieters, C. M. (1978) Mare basalt types on the front side of the moon: a summary of spectral reflectance data. *Ibid.* **9th**, 2825-50.
- (1982) Copernicus crater central peak: lunar mountain of unique composition. *Science* **215**, 59-61.
- (1986) Composition of the lunar highland crust from near-infrared spectroscopy. *Rev. Geophys.* **24**, 557-78.
- Hawke, B. R., Gaffey, M. and McFadden, L. A. (1983) Possible lunar source areas of meteorite ALHA81005: geochemical remote sensing information. *Geophys. Res. Lett.* **10**, 813-6.
- Adams, J. B., Mougini-Marx, P. J., Zisk S. H., Smith, M. G., Head, J. W. and McCord, T. B. (1985) The nature of crater rays: the Copernicus example. *J. Geophys. Res.* **90**, 12393-413.
- Head, J. W., Patterson, W., Pratt, S., Garvin, J., Barsukov, V. I., Basilevsky, A. T., Khodakovsky, I. L., Panfilov, A. S., Gektin, Yu. M. and Narayeva, Y. M. (1986) The color of the surface of Venus. *Science* **234**, 1379-83.
- Rossmann, G. R. (1980) Pyroxene spectroscopy. In *Pyroxenes* (C. T. Prewitt, ed.) *Rev. Mineral.* **7**, 91-115.
- Roush, T. L. and Singer, R. B. (1986) Gaussian analysis of temperature effects on the reflectance spectra of mafic minerals in the 1- μ m region. *J. Geophys. Res.* **91**, 10301-8.
- Runciman, W. A., Sengupta, D. and Marshall, M. (1973a) The polarized absorption spectra of iron in silicates. I. Enstatite. *Am. Mineral.* **58**, 444-50.
- and Gourley, J. T. (1973b) The polarized absorption spectra of iron in silicates. II. Olivine. *Ibid.* **58**, 451-6.
- Sherman, D. M., Burns, R. G. and Burns, V. M. (1982) Spectral characteristics of the iron oxides with application to the Martian bright region mineralogy. *Proc. Lunar Planet. Sci. Conf.*, **12th**, *J. Geophys. Res.* **87**, 100169-180.
- Singer, R. B. (1981) Near-infrared spectral reflectance of mineral mixtures: Systematic combinations of pyroxenes, olivines, and iron oxides. *J. Geophys. Res.* **86**, 7967-82.
- (1985) Spectroscopic observations of Mars. *Adv. Space Res.* **5**, 59-68.
- and Roush, T. L. (1985) Effects of temperature on remotely sensed mineral absorption features. *J. Geophys. Res.* **90**, 12434-44.
- McCord, T. B., Clark, R. N., Adams, J. B. and Huguenin, R. L. (1979) Mars surface composition from reflectance spectroscopy: a summary. *Ibid.* **84**, 8415-26.
- Smith, J. V. (1979) Mineralogy of the planets: a voyage in space and time. *Mineral. Mag.* **43**, 1-89.
- Smith, W. C. (1969) Arthur Francis Hallimond (1890-1968). *Ibid.* **37**, 313-6.
- Solberg, T. C. and Burns, R. G. (1988) Mössbauer spectra of weathered stony meteorites relevant to oxidation on Mars. I. Chondrites. II. Achondrites and SNC meteorites. *Lunar Planet. Sci. XIX*, 146-7 and 1103-4.
- Steffen, G., Langer, K. and Seifert, F. (1988) Polarized absorption spectra of synthetic (Mg, Fe)-orthopyroxenes, ferrosilite and Fe³⁺-bearing ferrosilite. *Phys. Chem. Minerals*, **16**, 120-9.
- Sung, C.-M., Abu-Eid, R. M. and Burns, R. G. (1974) Ti³⁺/Ti⁴⁺ ratios in lunar pyroxenes: implications to depth of origin of mare basalt magma. *Proc. Lunar Sci Conf.*, **5th** **1**, 717-26.
- Singer, R. B., Parkin, K. M. and Burns, R. G.

- (1977) Temperature dependence of Fe^{2+} crystal field spectra: implications to mineralogical mapping of planetary surfaces. *Ibid.* *8th*, 1063–79.
- Vaughan, D. J. and Burns, R. G. (1973) Low oxidation states of Fe and Ti in the Apollo 17 orange soil. *EOS Trans., AGU* **54**, 618–20.
- and Burns, R. G. (1977) Electronic absorption spectra of lunar minerals. *Phil. Trans. R. Soc. London A.* **285**, 249–58.
- White, W. B. and Keester, K. L. (1966) Optical absorption spectra of iron in the rock-forming silicates. *Am. Mineral.* **51**, 774–91.

[Manuscript received 16 March 1988: revised 20 June 1988]